

AD-A041 913

ROCHESTER UNIV N Y DEPT OF CHEMISTRY

F/G 7/4

THE STRUCTURE OF WATER DIMER FROM MOLECULAR BEAM ELECTRIC RESON--ETC(U)

SEP 76 T R DYKE, K M MACK, J S MUENTER

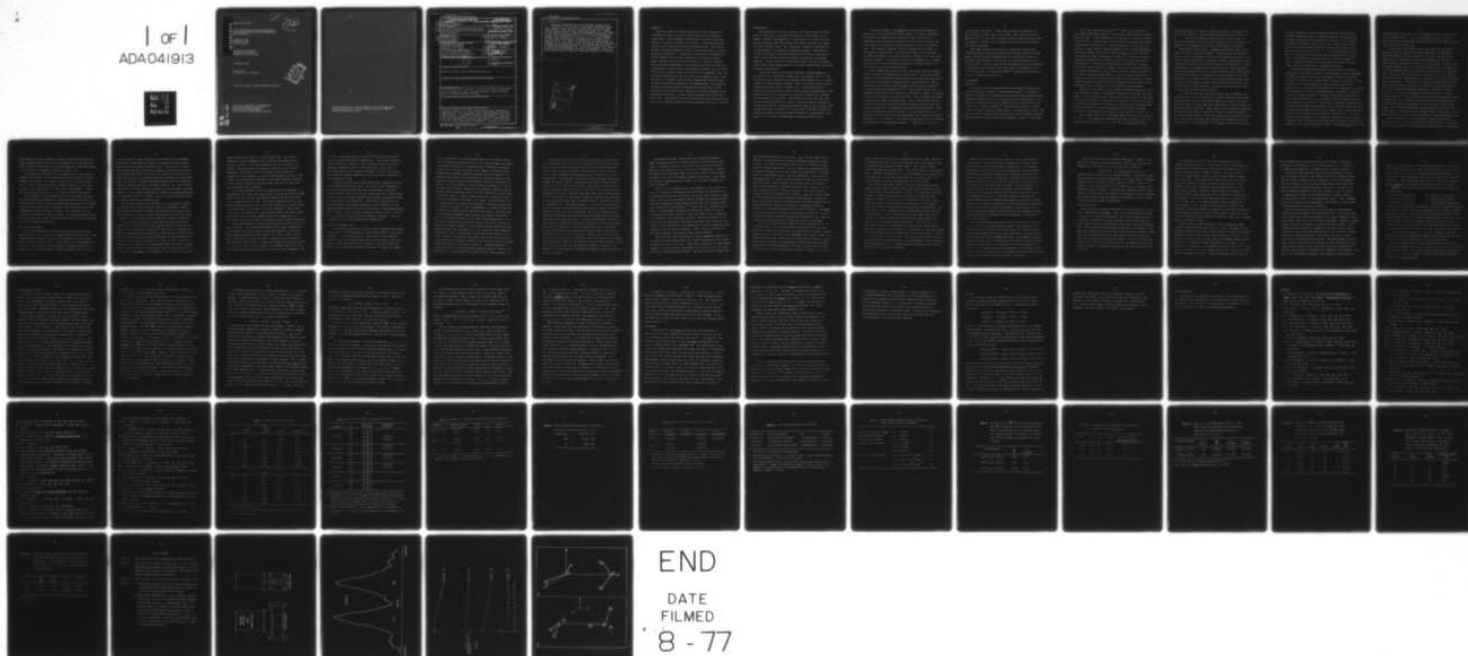
F19628-75-C-0063

UNCLASSIFIED

AFGL-TR-76-0216

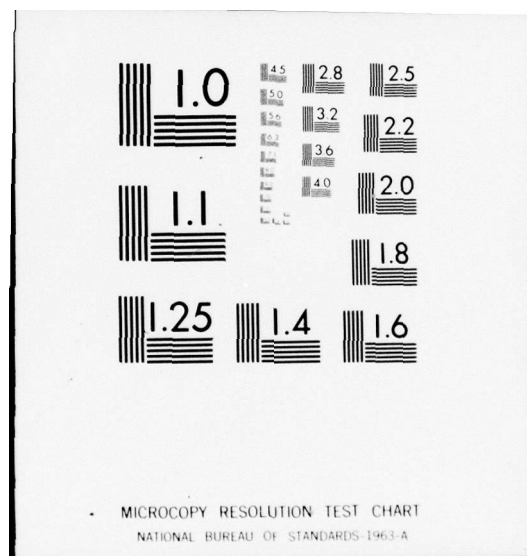
NL

1 of 1
ADA041913



END

DATE
FILMED
8-77



AD A041913

AFGL-TR-76-0216

THE STRUCTURE OF WATER DIMER FROM
MOLECULAR BEAM ELECTRIC RESONANCE
SPECTROSCOPY

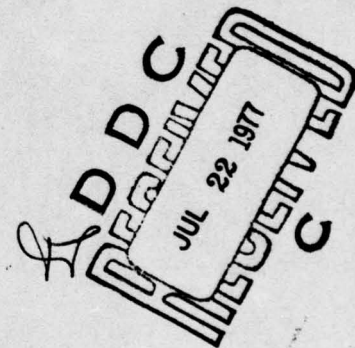
Thomas R. Dyke
Kenneth M. Mack
John S. Muentner

Department of Chemistry
University of Rochester
Rochester, New York 14627

1 September 1976

Final Report
November 1974 - June 1976

Approved for public release; distribution unlimited



AD No. _____
DDC FILE COPY

AIR FORCE GEOPHYSICS LABORATORY
AIR FORCE SYSTEMS COMMAND
UNITED STATES AIR FORCE
HANSCOM AFB, MASSACHUSETTS 01731

Qualified requestors may obtain additional copies from the Defense Documentation Center. All others should apply to the National Technical Information Service.

Unclassified

SECURITY CLASSIFICATION OF THIS PAGE (When Data Entered)

19 REPORT DOCUMENTATION PAGE		READ INSTRUCTIONS BEFORE COMPLETING FORM
1. REPORT NUMBER AFGL-TR-76-0216	2. GOVT ACCESSION NO.	3. RECIPIENT'S CATALOG NUMBER 9
4. TITLE (and Subtitle) THE STRUCTURE OF WATER DIMER FROM MOLECULAR BEAM ELECTRIC RESONANCE SPECTROSCOPY.		5. TYPE OF REPORT & PERIOD COVERED Final rept. Nov 1974 - 30 Jun 1976
7. AUTHOR(s) Thomas R. /Dyke Kenneth M. /Mack John S. /Muentert		8. CONTRACT OR GRANT NUMBER(s) F19628-75-C-0063, <i>see</i> NSF-MPS-74-12250
9. PERFORMING ORGANIZATION NAME AND ADDRESS Department of Chemistry University of Rochester Rochester, N.Y. 14627		10. PROGRAM ELEMENT, PROJECT, TASK AREA & WORK UNIT NUMBERS 61102F 86030301 1243
11. CONTROLLING OFFICE NAME AND ADDRESS Air Force Geophysics Laboratory Hanscom AFB, Massachusetts 01731 Monitor/Shepard A. Clough/OPI		12. REPORT DATE 1 September 1976
14. MONITORING AGENCY NAME & ADDRESS (if different from Controlling Office) 1259p.		13. NUMBER OF PAGES 56
		15. SECURITY CLASS. (of this report) Unclassified
		15a. DECLASSIFICATION/DOWNGRADING SCHEDULE
16. DISTRIBUTION STATEMENT (of this Report) Approved for public release; distribution unlimited.		
17. DISTRIBUTION STATEMENT (of the abstract entered in Block 20, if different from Report)		
18. SUPPLEMENTARY NOTES *Present address: Dept of Chemistry, Univ of Oregon, Eugene, Oregon 97403 Research supported by AFGL, Contract F19628-75-C-0063 and National Science Foundation Grant MPS-74-12250.		
19. KEY WORDS (Continue on reverse side if necessary and identify by block number)		
20. ABSTRACT (Continue on reverse side if necessary and identify by block number) Molecular beams of hydrogen bonded water dimer, generated in a supersonic nozzle, have been studied using electric resonance spectroscopy. Radio frequency and microwave transitions have been observed in (H ₂ ¹⁶ O) ₂ , (D ₂ ¹⁶ O) ₂ , and (H ₂ ¹⁸ O) ₂ . Transitions arising from both pure rotation and rotation-tunneling occur. The pure rotational transitions have been fit to a rigid rotor model to obtain structural information. Information on the		

DD FORM 1 JAN 73 1473

EDITION OF 1 NOV 65 IS OBSOLETE

Unclassified

SECURITY CLASSIFICATION OF THIS PAGE (When Data Entered)

307 260

4B

Unclassified

SECURITY CLASSIFICATION OF THIS PAGE(When Data Entered)

20. relative orientation of the two monomer units is also contained in the electric dipole moment component along the A inertial axis, μ_a , which is obtained from Stark effect measurements. The resultant structure is that of a "trans-linear" complex with an oxygen-oxygen distance, R_{OO} , of 2.98(1) Å, the proton accepting water axis is 58(6)° with respect to R_{OO} , and the proton donating water axis at -51(6)° with respect to R_{OO} . This structure is consistent with a linear hydrogen bond and the proton acceptor tetrahedrally oriented to the hydrogen bond. The limits of uncertainty are wholly model dependent and are believed to cover variations from the zero-point vibrational structure observed to the equilibrium structure. μ_a shows strong dependence on J and K and is about 2.6D. Centrifugal distortion constants have been interpreted in terms of the monomer-monomer stretching frequency and give $\omega = 150/\text{cm}^{-1}$.

degrees

The A component of electric dipole moment

omega

ADDITIONAL	
NTIS	White Section <input checked="" type="checkbox"/>
DOC	Buff Section <input type="checkbox"/>
UNANNOUNCED	<input type="checkbox"/>
JUSTIFICATION	<input type="checkbox"/>
BY	
DISTRIBUTION/AVAILABILITY CODES	
Dist.	Avail. and/or SPECIAL
A	

Unclassified

SECURITY CLASSIFICATION OF THIS PAGE(When Data Entered)

ABSTRACT

Molecular beams of hydrogen bonded water dimer, generated in a supersonic nozzle, have been studied using electric resonance spectroscopy. Radio frequency and microwave transitions have been observed in $(\text{H}_2^{16}\text{O})_2$, $(\text{D}_2^{16}\text{O})_2$, and $(\text{H}_2^{18}\text{O})_2$. Transitions arising from both pure rotation and rotation-tunneling occur. The pure rotational transitions have been fit to a rigid rotor model to obtain structural information. Information on the relative orientation of the two monomer units is also contained in the electric dipole moment component along the A inertial axis, μ_a , which is obtained from Stark effect measurements. The resultant structure is that of a "trans-linear" complex with an oxygen-oxygen distance, R_{00} , of 2.98(1) Å, the proton accepting water axis is 58(6)° with respect to R_{00} , and the proton donating water axis at -51(6)° with respect to R_{00} . This structure is consistent with a linear hydrogen bond and the proton acceptor tetrahedrally oriented to the hydrogen bond. The limits of uncertainty are wholly model dependent and are believed to cover variations from the zero-point vibrational structure observed to the equilibrium structure. μ_a shows strong dependence on J and K and is about 2.6D. Centrifugal distortion constants have been interpreted in terms of the monomer-monomer stretching frequency and give $\omega = 150 \text{ cm}^{-1}$.

INTRODUCTION

The structure of liquids in general, and the structure of liquid water in particular, have been the subject of a vast amount of research. However, the complexity of the problem is so great that only initial successes have been achieved and liquid structure will remain an active research field. The traditional approach to the structure of liquid water is to consider a macroscopic sample. Experimental studies have applied many spectroscopic and diffraction techniques to water, as well as most classical physical and chemical measurement methods.¹ A great variety of theoretical models have been applied to liquid water ranging from mixtures of ice-like crystallites to molecular dynamics calculations.²

In the past several years there has been a growing emphasis on approaching the liquid water problem from a microscopic point of view. The focus of this approach is the hydrogen bond between two, or a small number, of isolated water molecules. Thus, the species studied are hydrogen bonded water dimers, trimers, etc. A detailed knowledge of these isolated systems will provide a more complete understanding of the hydrogen bond and of intermolecular potential functions that dominate the structure of liquid water. Such studies of water and other small hydrogen bonded systems³ will lead to a much more general knowledge of all hydrogen bonding. The detailed study of systems such as water dimer should, therefore, contribute to a wide range of chemical problems including structure of condensed phases, solvation, intramolecular structure, and many areas of biochemistry involving hydrogen bonding.

A very large number of ab initio and semi-empirical quantum calculations have been performed on water dimer.⁴ As these calculations have become more sophisticated and contain fewer restrictions, a consensus on the theoretical structure of water dimer has arisen. The lowest energy equilibrium structure calculated is the "trans-linear" form. This structure contains a plane of symmetry and a linear, or near linear, hydrogen bond. A much smaller number of calculations have been performed on the trimer and larger polymers and no structural consensus exists.⁵ In particular, there is no agreement as to whether the trimer is an open structure containing two hydrogen bonds, or a cyclic entity with three hydrogen bonds.

From an experimental point of view, water dimers were first postulated to explain PVT observations on water vapor.⁶ Since the initial concept of isolated hydrogen bonded species, there have been many direct and indirect experimental investigations of these molecules. Water dimers have been directly observed using matrix isolation infrared^{7,8} and mass spectrometer techniques.^{9,10,11} The initial infrared work of Pimentel and coworkers⁷ was interpreted in terms of a symmetric structure containing two strongly bent hydrogen bonds. This conclusion was based on the observed number of normal modes. Later infrared work⁸ has obtained more data and concluded the dimer structure was more open with a single hydrogen bond, in agreement with theoretical predictions. While mass spectroscopy is normally insensitive to structural details, an electric deflection study of water dimer showed the symmetric structure of Pimentel is not correct.¹¹ Preliminary communications on the microwave spectroscopic work reported here showed water dimer to have the

"trans-linear" structure.¹² Much less experimental information on the structure of water trimer is available. The electric deflection observation¹¹ of a very small permanent electric dipole for the trimer is, however, a strong piece of evidence favoring the three hydrogen bond cyclic structure.

This paper presents the details of a molecular beam electric resonance study of the radio frequency and microwave spectra of water dimer. The spectroscopic observations are interpreted in terms of a quantitative geometric structure for the ground vibrational state of water dimer. Electric dipole moment measurements are also presented. The nonrigid nature of water dimer adds several complexities to its rotational spectra. The preceding paper^{12a} discusses the theoretical aspects of this nonrigid behavior.

EXPERIMENTAL

Apparatus

A molecular beam of hydrogen bonded water dimer was formed by expanding water vapor through a simple pinhole nozzle.¹³ Nozzles of different diameters and thicknesses were investigated and optimum dimer beams were produced using 0.1 mm diameter and 0.13 mm thickness. The nozzle was fabricated by using a jeweler's drill to place the hole in nickel foil of chosen thickness.¹⁴ The foil was sealed to a conventional beam source using an indium gasket. A skimmer was not used. However, a liquid nitrogen cooled cryopump with a one centimeter aperture for the beam was located about two centimeters in front of the nozzle.

As has been reported previously,^{11,12} this type of beam source can produce large water clusters if relatively high pressures of water vapor are used. At one atmosphere source pressure, all $(\text{H}_2\text{O})_n$ clusters within the $m/e = 350$ mass limit of the molecular beam mass spectrometer detector have been observed.¹¹ Optimum production of dimers was observed at roughly 100 torr source pressure and 80°C source temperature. The source pressure has not been directly measured but was adjusted to maximize the dimer concentration in the beam. The dimer content of the beam was monitored at the H_3O^+ ion peak of the mass spectrometer beam detector. Since higher polymers also contribute H_3O^+ fragment ions, dimer concentration was judged by observing only those molecules which were focused around a beam stop by the state selecting fields of the electric resonance spectrometer. Since the higher polymers are essentially nonpolar¹¹ they were not focused into the detector. Under standard operating conditions the H_3O^+ ion peak from water dimer was approximately 10% as intense as the H_2O^+ peak from water monomer.

Because it was necessary to use rather low source pressure to avoid higher polymer formation, the absolute intensity of the dimer beam was small. The low source pressure also meant the nozzle was not operating far into the supersonic region and little cooling of rotational degrees of freedom was observed.¹⁵ Therefore, a relatively weak molecular beam with a large partition function was used and individual rotational transitions were observed with relatively poor signal to noise ratio.

$(\text{H}_2\text{O})_2$ beams were formed from normal water¹⁶ and were monitored at $m/e = 19$. $(\text{D}_2\text{O})_2$ beams were generated from 99% enriched D_2O vapor and were detected at D_3O^+ , $m/e = 22$. A 93% ^{18}O enriched sample of H_2O ,

kindly provided by Dr. Pinchas of Weizman Institute, was used to produce $(\text{H}_2^{18}\text{O})_2$ species. These molecules were observed at $\text{H}_3^{18}\text{O}^+$ at $m/e = 21$. One day of operation required several grams of water so fairly large amounts of material were required. Most of the water is trapped on the cryopump and the small H_2^{18}O sample was recycled.

The molecular beam electric resonance spectrometer used in this study has been previously described.¹⁷ Modifications not discussed earlier include the molecular beam source, microwave electronics, and signal averaging capability. Microwave radiation, generated by reflex klystron oscillators, was introduced into the resonance region of the spectrometer by a waveguide which extends up to the electrodes which provide the uniform Stark field. These electrodes (the C-field) allow the microwave radiation to propagate from the waveguide to the beam molecules. In a nearly prolate rotor with the K quantum number equal to zero it is desirable to observe $\Delta M=0$ transitions and in this case the broad wall of the waveguide is parallel to the beam axis to make the radiation and static fields parallel.

It is not obvious that rotational transitions in symmetric top molecules with $K>0$ can be observed in electric resonance spectroscopy. The requirement that the Stark coefficient of the initial and final level be greater and less than zero, respectively, certainly cannot be met with parallel radiation. Water dimer a-type rotational transitions with $K\geq 2$ are essentially identical to those of a perfect symmetric top since the Stark shift is typically larger than the asymmetry splitting. Such transitions have been observed with perpendicular microwave radiation. The feasibility of this type of transition was ascer-

tained by observing virtually identical rotational transitions in the O_2^{20} vibrational state of carbonyl sulfide.¹⁸ The observation of these transitions can be explained in two ways. It is possible to observe a transition from a level with a positive Stark coefficient to a level with essentially zero Stark coefficient and thus the transition can be $M = 1 \rightarrow M' = 0$. It is also possible to start with $M > 0$ and achieve $M' < 0$ levels by inducing multiple $\Delta M = 1$ transitions, each transition reducing M by one, to cause a cascade of $\Delta M \gg 1$. Since observations were always made with excess microwave power, the latter explanation is probably important.

Several different procedures were used in measuring microwave transitions. For initial searches it was desirable to have linewidths as large as possible and this was achieved by frequency modulating the radiation source with random noise.¹⁹ Since the radiation was not detected, this technique does not lower the sensitivity of the spectrometer as long as sufficient power per unit bandwidth is available. With approximately 100 mw of microwave power, linewidths in excess of 10 MHz were readily achieved. Convenient modulation is obtained by mechanically switching the noise voltage, which is applied to the klystron repeller, on and off at a 10 Hz rate. Transition frequencies can be measured to 10 MHz accuracy using a cavity frequency meter and 1 MHz accuracy was obtained by observing zero beating with a known frequency during the half modulation cycle when the noise was off. For higher resolution measurements it was necessary to phase lock the klystron to a stable frequency derived from a crystal oscillator and frequency synthesizer. The linewidth observed is about 30 KHz FWHM which results from

unresolved hyperfine structure and non-optimum radiation distribution in the resonance region. Initial measurements were made using frequency modulation accomplished by modulating the 30 MHz reference oscillator of the phase locked loop.

It was difficult to maintain phase lock and adequate frequency deviation and still sweep the microwave frequency. An amplitude modulator capable of 100% modulation at 10 Hz over the 8-60 GHz frequency region is necessary to simplify measurements of this kind. A simple mechanical modulator was built for this purpose. A short length of X-band waveguide was fitted with an oscillating vane connected to a small shaft passing through the center of the narrow wall of the waveguide. When this vane is parallel to the broad wall in the middle of the waveguide it is perpendicular to the microwave E field and causes minimum attenuation. Rotation of the vane shaft approximately 20 degrees brings the edges of the vane in contact with the broad walls of the guide, blocking microwave transmission. The shaft is made to oscillate at 10 Hz by a galvanometer drive manufactured for optical scanning mirrors.²⁰ Cross sectional sketches of the modulator are shown in figure one. Using tapered transition sections this modulator can be used for frequencies throughout the usual microwave spectroscopic region. With this modulator phase locked klystrons were stable and easily swept. Signal averaging was accomplished by interfacing a multi-channel analyzer to the frequency synthesizer in the phase locked loop.

Radio frequency, RF, transitions were observed by generating suitable radiation fields both parallel and perpendicular to the static field. The RF source is a Hewlett-Packard 3330A frequency synthesizer.

The frequency range is extended by harmonic generation and filtering using a Hewlett-Packard 10511A spectrum generator and 230B amplifier. Radio frequency transitions are 10-30 KHz FWHM due to unresolved hyperfine structure. Instrumental linewidth is about 3 KHz.

The frequencies reported are the average of data taken sweeping frequency up and down. Most measurements were made using a 30 second detector time constant with signal to noise ratios varying between 5 and 20. Signal averaging was used to improve signal to noise ratios for some lines, particularly for Stark effect measurements. Figure 2 shows signal averaged results for two radio frequency transitions.

The assignment of many microwave lines was confirmed by RF-microwave double resonance experiments. These experiments were most frequently carried out by fixing the modulated RF frequency at an assigned transition and monitoring the intensity of this RF transition as the unmodulated microwave frequency is swept. The intensity of the RF transition is observed to either increase or decrease, depending on the relative energy level scheme, when both transitions occur simultaneously and involve a common energy level.

Preliminary Discussion

All of the spectroscopic transitions we have observed in water dimer fall into one of two groups. Many transitions clearly arise from a nearly prolate symmetric top rotor with permanent electric dipole moment component parallel to the A axis, which is the approximate prolate axis. The remaining transitions show no apparent pattern and will not fit a rigid rotor model. As was discussed in detail in the

previous paper,^{12a} these observations are consistent with hydrogen bonded water dimer molecules capable of undergoing proton tunneling motions which interchange identical nuclei. The majority of microwave transitions will involve both rotational and tunneling energies. It was shown that there are at least six tunneling splittings of unknown magnitude and the resultant spectrum is indeed very complicated. There are, however, allowed transitions between two of the tunneling sublevels which only involve rotational energies, i.e., these transitions connect the same tunneling sublevels in two different rotational states. The two tunneling sublevels in question are doubly degenerate with symmetry E^+ and E^- . Figures 3 and 4 of the previous paper show the allowed transitions for water dimer.

The picture of water dimer undergoing large amplitude tunneling motions was not available when this study was undertaken. Rather, this model was developed to explain the observed spectroscopic data. This approach was, however, greatly facilitated by the earlier study of hydrogen fluoride dimer which was observed to exhibit tunneling.³

The frequencies obtained from the pure rotational transitions between the E states can be fit with conventional rigid rotor theory using effective rotational constants.²² Water dimer is necessarily a slightly asymmetric prolate top since it contains only two heavy atoms. The A inertial axis will be nearly coincident with the oxygen-oxygen axis for any structure of the molecule. The A, B, and C rotational constants can be estimated from approximate structures based on oxygen-oxygen distances obtained from studies of ice²³ or liquid water,²⁴ or structures from ab initio or semi-empirical calculations can be used.⁴

Rough estimates are $A \approx 2 \times 10^5$, $B \approx 6 \times 10^3$, $C \approx 6 \times 10^3$ MHz. The degree of asymmetry is highly dependent on B-C which is determined by fine structural details. B-C can be expected to be in the range of 0 to 100 MHz. Thus the molecule is strongly prolate and only slightly asymmetric. The vector sum of the monomer dipole moments will guarantee a large component of electric dipole moment parallel to the A axis. The perpendicular component of the moment depends critically on the relative orientation of the monomer units and can vary from zero to greater than two Debyes.

With these estimates, rigid rotor spectra can be calculated. In the symmetric top limit, the energy levels are given by $BJ(J+1) + (A-B)K^2$ where J and K specify the total angular momentum and the projection of that momentum on the A axis. Transitions associated with μ_a , the dipole moment parallel to the A axis, are referred to as A type transitions and change J by one unit and leave K unchanged. These transitions occur at 2B, 4B, 6B, etc. Perpendicular moment transitions change both J and K and the lowest frequency one is at approximately A or 2×10^5 MHz. This is well above the frequency range of these experiments.

The slight asymmetry of the molecule splits each $K > 0$ level into a pair of levels. The average frequencies of the A type transitions between these split levels, within a good approximation, are given by the average rotational constant $(B+C)/2$, i.e. $(B+C)$, $2(B+C)$, $3(B+C)$, etc. More accurate average rotational constants can be obtained by applying small corrections.²⁵ Transitions between the two split levels of a single J state are also allowed. The asymmetry splittings (and also these transition frequencies) are strongly J and K dependent. For

K=1 and 2, these splittings are given by²⁶ $(B-C)J(J+1)$ and $(B-C)^2 (J-1)J(J+1)(J+2)/[16(2A-B-C)]$ respectively. Water dimer should exhibit, therefore, a series of radio frequency transitions for K=1 asymmetry doublets in the 10 to 1000 MHz range, and in the 0.1 to 100 MHz range for K=2 asymmetry doublets. For K>2, the transitions between asymmetry splittings will be too small to observe for any reasonable J value.

Several conclusions about water dimer radio frequency and microwave transitions should be noted. The strong J and K dependence of the radio frequency transitions make quantum number assignment a trivial process. None of the A type transitions have a useful dependence on the A rotational constants and structure determination must be made without this information. Stark effect measurements on A type transitions will depend dominantly on the A component of the permanent dipole moment which is nearly parallel to the oxygen-oxygen axis. Finally, each of the two tunneling states, E^+ and E^- , will exhibit slightly different effective rotational constants. This can be thought of as a vibration-rotation interaction.²²

Transition Frequency Data

The first data consisted of a set of radio frequency transitions in the range of 1-10 MHz which fit to the fourth power of the angular momentum; $\nu = c(J-1)(J)(J+1)(J+2)$. This portion of the spectrum clearly arises from asymmetry splittings for K=2 levels. The coefficient c in the above expression is equal to $[(B-C)^2/16(2A-B-C)] + D_3$ where D_3 is a centrifugal distortion constant.²⁷ While this combina-

tion of constants is not particularly useful for structural information, the absolute certainty of the J and K quantum number assignment is extremely important for identifying pure rotational transitions. A second set of transitions between K=2 asymmetry doublets having a substantially different asymmetry parameter was also observed. As previously described, these two groups of transitions belong to two separate tunneling levels having different effective rotational constants. It is not possible to assign which set belongs to E^+ and E^- representations and the transitions are therefore labeled E_1 and E_2 . The data and corresponding values for the c coefficient for H_2O dimer are given in table 1. Similar results have been obtained for $(D_2O)_2$ and this information is included in the table. The coefficient c is not constant with J but shows some additional centrifugal distortion as indicated in figure 3. This J dependence is a smooth function and indicates the expected smaller distortion for $(D_2O)_2$. The magnitude of the asymmetry parameter would, however, increase on deuteration for a rigid molecule contrary to the water dimer observations. It is difficult to know how to divide the origin of this fact, as well as the large difference between c for E_1 and E_2 states, between the rotational constant and D_3 portions of c. For the usual rigid asymmetric top molecule, the D_3 contribution to this coefficient would be very small. However, the expected very small value of B-C and the large A value minimize the rotational constant term while the low force constant vibrational modes of water dimer enhance D_3 . Anomalous behavior of this coefficient has been previously observed in HSSH.²⁸ Without K=1 information it is not possible to separate the two contributions.

Structural data is best obtained from the pure rotational microwave transitions. To select the desired rotational transitions associated with the E tunneling levels from the rotation-tunneling transitions, double resonance techniques were employed. The $J=2, K=2$ to $J=3, K=2$ pure rotational transitions will be at $6(B+C)/2$, or in the 36 GHz range. The microwave transitions in this frequency region were checked for double resonance connections with radio frequency transitions for $J=2, K=2$ and $J=3, K=2$ levels. Since some of the radio frequency asymmetry doublets for the $J=2, K=2$ and $J=3, K=2$ states are inaccessible, the double resonance experiments were done in the presence of an electric field, E. The radio frequency transitions were observed in the strong field limit where the Stark effect is linear²⁹ and given by $-\mu_i EMK/[J(J+1)]$. The dipole moments, μ_i , of the two E states are slightly different and sufficiently large electric fields were used to separate the two pure Stark transitions. All of the required double resonance connections were found and the two microwave pure rotational transitions were thus identified. All that remained was to identify which microwave transition correlated to which set of zero field asymmetry doublet transitions. This information was lost in the double resonance experiment because the high field pure Stark transitions do not depend on the zero field splitting. However, the correlation was easily established by the fact that the zero field microwave transitions have observable K doubling. By tracking the high field microwave transition to zero field and then measuring the asymmetry splitting, one obtains the correct identity of asymmetry parameter, microwave frequency, and dipole moment.

The appropriate Stark coefficients also confirm the quantum number assignment and pure rotational nature of the microwave transitions. In addition, the $J=3, K=2$ to $J=4, K=2$ transitions were observed at four thirds the $J=2, K=2$ to $J=3, K=2$ frequencies. Similar measurements have also been made on D_2O dimer. Table 2 lists average frequencies for the $K=2$ K doublet microwave transitions. Also listed are corrected frequencies which account for the small asymmetry of the K doublets.²⁵

The $J=3$ to $J=4$ transitions are not precisely at four thirds the $J=2$ to $J=3$ transition frequencies and this allows the evaluation of a D_J centrifugal distortion coefficient for the E_1 and E_2 states of water dimer. This constant can then be used to estimate the monomer-monomer stretching frequency by approximating water dimer as a diatomic molecule consisting of two monomers.³⁰ In this case, $D_J = 4[(B+C)/2]^3/\omega^2$ where ω is the harmonic stretching frequency and $(B+C)/2$ is used as the average rotational constant. While this model is very simplistic it is expected to be relatively accurate. The main deficiency is ignoring angular vibrational coordinates with small force constants, but $(B+C)/2$ is most sensitive to the separation of the two oxygen atoms and, therefore, the stretching coordinate. Table 3 lists D_J and this vibrational frequency for the water dimer species studied.

While the zero field splittings of the $K=3$ asymmetry doublets are too small for direct observation, pure Stark transitions can be observed and identified with $K=3$ states. Using these transitions of known quantum numbers in double resonance experiments, the $J=3, K=3$ to $J=4, K=3$ pure rotational transitions were assigned. This provides data to obtain the

D_{JK} centrifugal distortion coefficient. D_{JK} is rather large, as expected for a molecule with low energy vibrational modes and a large A value. $K=3$ states have greater than 50 cm^{-1} of rotational energy about the oxygen-oxygen axis. D_{JK} is an important parameter because it allows the prediction of low K rotational transitions. This minimizes the experimental search, but more importantly, the accuracy of the predictions is a measure of the validity of using the rigid rotor plus centrifugal distortion model to interpret water dimer spectra. The $K=3$ pure rotational transition data are given in table 2. The $K=2$ and 3 microwave data for $(\text{H}_2^{16}\text{O})_2$ and $(\text{D}_2\text{O})_2$ were used to predict similar transition frequencies for $(\text{H}_2^{18}\text{O})_2$. Using the limited supply of ^{18}O enriched water these transitions were observed. Because of sample limitations only low resolution noise broadened spectra were obtained and double resonance verification of assignments was not feasible. The observed frequencies are listed in table 2. Assignment uncertainties exist for the $K=2$, E_2 transitions and the $K=3$, E_1 and E_2 designation could be reversed producing only changes in D_{JK} . These uncertainties do not affect use of these data later in this paper.

Only one possible ambiguity remains in the assignment of $K=2$ and 3 microwave data. For $K=2$ transitions it was proven that the lower frequency microwave data belongs to E_1 states while the higher frequency transitions are in E_2 states. The assignment of $K=3$ data in table two assumes the same order. Reversing the order does not yield D_{JK} values of particularly unreasonable magnitude but these constants do predict unreasonable rotational constants, $(B+C)_{00}/2$, for the $J=0$, $K=0$ rotationless state. Using the assignment in table 2 $(B+C)_{00}/2$ for the E_1

and E_2 states are very similar, differing by about 2.5 MHz. This is the expected behavior of non-rigid molecules and is the observed case in ammonia²² and hydrogen fluoride dimer.³ The alternate choice yields constants over 40 MHz apart. This latter result is not acceptable. Absolute confirmation of E state assignments can be obtained by the observation of microwave transitions for a third K state. For several reasons, the most desirable data is for K=0 states.

The second order Stark effect¹⁹ of the K=0 transitions requires greater focusing field voltages which significantly reduce the signal to noise ratio of the spectrometer. However, the prediction from the higher J, K transitions proved to be accurate to within one half megahertz for the J=0, K=0 to J=1, K=0 transition, for the E_1 state. There are several rotation-tunneling transitions in this frequency region and careful confirmation of this assignment was necessary. The Stark effect of this transition was accurately measured and confirms the assignment. This is a particularly rigorous test since second order Stark effect requires that both the dipole moment matrix elements and the transition energies be correct. The J=1, K=0 to J=2, K=0 transition was also observed with a centrifugal distortion parameter, D_J , identical to the higher J, K determination. The Stark effect of this transition was also commensurate with the assignment. Finally, the J=1, K=0, M=0 to J=1, K=0, M=±1 pure Stark transition was observed with appropriate dipole moment and energy denominator. This transition was also observed to have a double resonance connection with the J=0, K=0 to J=1, K=0 microwave transition.

The $K=0$ data are also listed in table 2. Only E_1 transitions were observed. The E_2 transitions are masked by a stronger transitions arising from rotation-tunneling transitions. All microwave transitions in the 12 and 24 GHz regions which have been attributed to rotational-tunneling transitions have exhibited incorrect Stark effect for pure rotational transitions. The accidental overlap of a rotation-tunneling and a pure rotation transition is indicative of the complexity of the water dimer spectrum. At the instrument sensitivity required for the $K=0$ observations, rotation-tunneling transitions are extremely dense and the overlap in question is not an improbable occurrence. It has been extremely fortunate that molecular beam electric resonance spectroscopy can be used to easily observe radio frequency transitions, including pure Stark transitions, and make precise dipole moment measurements. This ability, along with straightforward double resonance capabilities between radio and microwave frequency transitions, has been essential in sorting out water dimer spectra.

Careful searches have been made in the 24 GHz region for the $J=1$, $K=1$ to $J=2$, $K=1$ transitions without success. This failure is, unfortunately, to be expected due to the presence of numerous lines in this frequency range which are not pure rotational in nature and the large uncertainty in the asymmetry doubling. The asymmetry doubling, which could range from 0 to 200 MHz, not only makes the search problem difficult but also determines the Stark effect and, therefore, determines many necessary experimental parameters. Much effort was expended in the $K=1$ searches since the asymmetry splitting would provide a value for B-C and very useful structural information.

The K=2 and 3 microwave transition frequencies in tables 2 have been fit to average rotational constants, $[(B+C)/2]_{00}$, for the rotationless J=0, K=0 state, D_J , and D_{JK} using the expression:

$$\nu(J, K \rightarrow J+1, K) = [(B+C) - 2K^2 D_{JK}] (J+1) - 4D_J (J+1)^3,$$

for each tunneling state of each isotopic species. The results, along with calculated vibrational frequencies are given in table 3. The most complete data set exists for the E_1 state of $(H_2^{16}O)_2$. Here it is possible to do a least squares fit to $[(B+C)/2]_{00}$, D_J , and D_{JK} . The results are given in table 4. The excellent agreement between table 3 and 4 is an additional confirmation of assignments and data treatment. Since the E_1 data is the most complete and reliable, it will be used in the following structure calculations.

Stark Effect Data

The Stark effect has been discussed in the previous section as an aid to spectroscopic assignment. Here it will be presented in terms of electric dipole moment measurement. The electric dipole moment is a molecular property of intrinsic interest, but in water dimer the dipole moment also plays an important role in the structure determination. This situation occurs because the dominant contribution to the water dimer moment is the vector sum of the two monomer moments. Therefore, the relative orientation of the monomer units is strongly reflected by the dimer electric dipole moment. In the next section the dipole moment data to be presented here will be combined with the rotational constant information to obtain the structural parameters for water dimer.

As mentioned previously, pure Stark transitions have been studied for states with $K \geq 2$. Linear Stark effect²⁹ occurs when the Stark energy is much larger than the zero field asymmetry splitting. For $K \geq 2$ this condition is readily achieved. The Stark energy is given by $-\mu_a EMK/[J(J+1)]$, where μ_a is the dipole moment component along the A axis. The transitions in question are $\Delta M=1$ and, therefore, the transition frequency is given by $\mu_a EK/[J(J+1)]$. For $(H_2^{16}O)_2$, this type of transition has been measured for $K=2,3,4$ in both E_1 and E_2 states. Since the dipole moment is different for the two E states, two transitions will be observed for sufficiently large fields. This will occur when $\Delta\mu_a EK/[J(J+1)]$ is greater than the linewidth, where $\Delta\mu$ is dipole moment difference between the E_1 and E_2 states. Figure 2 shows this situation for $J=2, K=2$. The essentially identical intensity of these two transitions requires very similar absolute energy for the E_1 and E_2 states. This fact, along with the observation of two and only two sets of transitions, strongly support the tunneling model.

Accurate data was obtained for $K=2,3$ and 4 states and double resonance experiments were used for the E_1 and E_2 assignment as previously described. The results, given in table 5, indicate significant dependence on both K and E state. While this data is unusual, it is not surprising as it will be shown that angle changes between monomer units of ± 0.5 degree will change the moment by ≈ 0.03 Debye. This sensitivity of moment with angle change, along with the 35 cm^{-1} energy difference between $K=2$ and $K=3$ states, makes large changes in observed moments the expected behavior. These measurements further show that

the K dependence of the dipole moments is not simple or monotonic. To observe any dependence on the J quantum number, J=2, K=2 and J=3, K=2 moments were measured. The small effect is shown in table 5.

K=2 and K=3 dipole moments have also been obtained for $(D_2O)_2$, and are listed in table 5. The moments for the two tunneling states are much closer together and the K dependence is also much smaller. This is consistent with $(D_2O)_2$ having both smaller zero point vibrational amplitudes and less centrifugal distortion. Because of the small difference between the two $(D_2O)_2$ moments it was not possible to unambiguously assign the observed moments to tunneling states. The assignment in table 5 is by analogy with $(H_2O)_2$. This assignment gives K and tunneling state dependence of the moment in $(D_2O)_2$ which is qualitatively the same as in $(H_2^{16}O)_2$.

The second order Stark effect for K=0 states is significantly different from the higher K first order effect.²⁹ In principle, the second order Stark coefficients depend on all three components of the dipole moment and also on the A rotational constant. However, in water dimer μ_a and $(B+C)/2$ dominate the second order Stark effect. In an attempt to obtain additional information, the Stark effect of three second order transitions were measured using long periods of computer averaging to improve precision. The results are given in table 6 for the three transitions involving K=0. The dipole moment values in table 6 were obtained from the experimental Stark coefficients using simple linear molecule second and fourth order Stark expressions.³¹ For K=0, this analysis is equivalent to a symmetric top treatment. The data is too correlated to attempt a full asymmetric top analysis to

obtain μ_b, μ_c and A values. The most useful approach is to consider only transitions which are allowed in the symmetric top limit and to include only the A rotational constant in energy denominators for ΔK transitions. These assumptions are fully justified by the precision of the data. Using this simplified approach, the μ_b and μ_c dipole moment components have identical contributions and we can define $\mu_{\perp} \equiv \sqrt{\mu_b^2 + \mu_c^2}$. The Stark coefficients for the three $K=0$ transitions are given below.

$J=0, K=0, M=0 \rightarrow J=1, K=0, M=0$	$\Delta\omega = [8\mu_a^2/15(B+C) + 2\mu_{\perp}^2/15A]E^2$
$J=1, K=0, M=0 \rightarrow J=1, K=0, M=\pm 1$	$\Delta\omega = [3\mu_a^2/10(B+C) + \mu_{\perp}^2/5A]E^2$
$J=1, K=0, M=0 \rightarrow J=2, K=0, M=0$	$\Delta\omega = -[16\mu_a^2/105(B+C) + 4\mu_{\perp}^2/105A]E^2$

Note that the two microwave transitions, the first and third expressions, have identical moment dependence and should produce identical moments as listed in table 6. The observed difference stems in part from experimental uncertainty and in part from centrifugal distortion effects on the moments. Since the two data involving $J=0$ and $J=1$ energy levels are more precise and have less centrifugal distortion³² these can be used, along with a calculated A value, to obtain an estimate for μ_{\perp} . This produces a value of $\mu_{\perp} = .3 \pm .15D$. Because of uncertain centrifugal distortion effects this number is not reliable but this data does allow reliable upper limit of $0.6D$ to be placed on μ_{\perp} .

In the following section a more detailed discussion of the water dimer electric dipole moment will be given. This will include calculation of electrostatic interactions between monomers and quantitative description of the dimer moment in terms of the internal degrees of freedom of the dimer structure.

STRUCTURE CALCULATION

The basic structure of water dimer can be determined from experimental rotational constants from different isotopic species and from electric dipole moments. We employ a simple rigid rotor model to calculate the dimer moments-of-inertia in the principal axis system and a vector model, including corrections for induced moment and charge transfer effects, to account for the dimer electric dipole moment.

The principal moments of inertia for a given isotopic species of water dimer are calculated with the assumption that the monomer subunits have the same geometry as the equilibrium structure of the free water monomer³³ given in Table 7. Thus there are six unconstrained coordinates describing the orientation of the monomers in water dimer. These are conveniently described by the oxygen-oxygen internuclear distance, R_{OO} , and the Euler angles ϕ_d , θ_d , χ_d and ϕ_a , χ_a ($\phi_a \equiv 0$). The subscripts refer to the proton donating and proton accepting monomers. These six coordinates give the orientation of the donor and acceptor monomer molecules with respect to the reference configuration shown in Fig. 4a. The reference configuration is chosen so the C_2 axis of each monomer (the C_2 axis is assumed to point toward the oxygen atom) lies in the positive Z direction for $\phi_d = \theta_d = \phi_a = \theta_a = 0$. The χ_d and χ_a specify the rotation of the monomers about the C_2 axis with $\chi_d = 0$ placing the donor protons in the XZ plane and $\chi_a = 0$ placing the acceptor protons in the YZ plane. One of the azimuthal angles ϕ_a can be arbitrarily set equal to zero, fixing the C_2 axis of the acceptor to lie in the XZ plane. The "trans-linear" structure predicted by calculations is shown in Fig. 4b. This structure has an XZ plane of symmetry,

requiring $\chi_a = \chi_d = \phi_d = 0$ and a linear hydrogen bond, fixing $\theta_d = -\frac{1}{2}\alpha$, where α is the monomer bond angle.

To obtain initial structural parameters, the "trans-linear" structure of Fig. 4b was used. This initial assumption, which will be shown to be valid below, can be based on evidence from the structure of ice,²³ water dimer calculations,⁴ and experimental and theoretical results on other small hydrogen bonded systems.^{3,34} The most important constraint is the linear hydrogen bond. This configuration minimizes repulsions between non-hydrogen bonded protons and is a reasonable first choice.³⁵ The experimental evidence in its favor will also be presented below. From the $(\frac{B+C}{2})$ values for two different isotopic species, R_{OO} and θ_a can be calculated. The results are given in Table 8. From the average of the $(H_2^{16}O)_2/(D_2^{16}O)_2$ and $(H_2^{18}O)_2/(D_2^{16}O)_2$ results, $R_{OO} = 2.98 \text{ \AA}$ and $\theta_a = 58.8^\circ$. The $(H_2^{16}O)_2$ and $(H_2^{18}O)_2$ results give a much larger value for θ_a , 82.2° . However, relative differences in $\frac{B+C}{2}$ for $(H_2^{16}O)_2$ and $(H_2^{18}O)_2$ depend primarily on R_{OO} and the mass change, and only slightly on the orientations of the monomers. An error of 10 MHz in $\frac{B+C}{2}$, caused by model errors (since the experimental error is almost certainly a negligible factor in these calculations), could cause an error of 30° in θ_a if $(H_2^{18}O)_2/(H_2^{16}O)_2$ data are used (see appendix I). The corresponding error in θ_a from $(H_2O)_2/(D_2O)_2$ data would only be 3° . Thus the best results should be obtained from $(D_2O)_2/(H_2O)_2$ data, and simultaneous fits of $(H_2^{16}O)_2$ and $(H_2^{18}O)_2$ data to calculate geometries will not work well with a rigid rotor model.

To remove the constraint of a linear hydrogen bond, it is necessary to use a third experimental datum in addition to $\frac{B+C}{2}$ for two isotopic species. As discussed above, attempts to simultaneously fit $\frac{B+C}{2}$ for $(H_2^{16}O)_2$, $(H_2^{18}O)_2$ and $(D_2^{16}O)_2$ are likely to magnify model inaccuracies, and, in fact, no structure would fit all three values of $\frac{B+C}{2}$ to better than about 10 MHz. Fortunately, the A-component of the electric dipole moment, μ_a , depends strongly on θ_a and θ_d and can be used to determine θ_d . It is readily shown that μ_a is given by equation 1:

$$\mu_a = \mu[\cos\theta_a + \cos\theta_d] + [\mu_{ind}]_a + [\Delta\mu_{CT}]_a. \quad (1)$$

μ is the electric dipole moment of the free monomer, 1.855D,³⁶ $\Delta\mu_{CT}$ is the dipole moment enhancement caused by transfer of electronic charge from the proton acceptor to the proton donor molecule. μ_{IND} is the vector sum of the dipoles induced on each monomer by the electric field caused by the charge distribution of the other monomer. By using a multipole expansion for the electric field, the dipole and quadrupole-induced dipole moments can be calculated³⁷ and the results are given in table 9. The values of $[\mu_{ind}]_a$ for the structure given below is 0.42D. Since the multipole expansion may not rapidly converge at the water dimer internuclear separation, and because the charge-transfer term, although most likely small, may be significant, we also obtained ab initio values of the total enhancement of the dimer dipole moment due to charge-transfer and induced moment effects.³⁸ These results, found with a minimal basis set are given in Table 9, along with the electrostatic calculation results. Other ab initio calculations⁴ with much larger basis sets report total dipole moment enhancements in the range of 0.3-0.4D. All of these results predict a dipole moment enhancement of about $0.4 \pm .1$ debye. We have,

therefore, chosen to use the electrostatic calculation results, $0.42D$, with the very conservative uncertainty limits of $\pm 0.3D$. With this result Eq. 1 becomes

$$\mu_a = \mu[\cos\theta_a + \cos\theta_d] + 0.42 \pm 0.30 \quad (2)$$

The moment enhancement term has some dependence on θ_a and θ_d and Eq. 2 is valid for $\theta_a \approx 60^\circ$ and $\theta_d \approx -50^\circ$. In further support of Eq. 2, the enhancement of μ_a in $(HF)_2$, over that of the vector sum of monomer components is $0.56D$. Thus Eq. 2 is quite realistic.

Using Eq. 2 as a third constraint, along with $\frac{B+C}{2}$ for two isotopic species, R_{OO} , θ_a and θ_d can be determined. The results are presented in Table 10. R_{OO} and θ_a are almost unchanged from Table 8, and θ_d is within 2° of a linear hydrogen bond ($\theta_d = -52.26^\circ$ for a linear hydrogen bond).

The remaining constraints on the dimer geometry, $\chi_a = \chi_d = \phi_d = 0$, are more difficult to assess. χ_a and χ_d give the rotation of the monomers around their C_2 axes, and for a linear hydrogen bond, ϕ_d gives the torsional angle of H_3 , in Fig. 4b, out of the plane of the drawing. Thus it is reasonable, and the calculations given in Table 11 show that $\frac{B+C}{2}$, which depends strongly on R_{OO} , θ_a and θ_d , depends weakly on χ_a , χ_d and ϕ_d . The good aspect of this is that our values of R_{OO} , θ_a and θ_d are almost independent of our choice of $\chi_a = \chi_d = \phi_d = 0$. However, since μ_a is affected by χ_a , χ_d and ϕ_d only slightly (the enhancement term of Eq. 2 depends on them), and at least for the isotopic species studied so far, $\frac{B+C}{2}$ is only weakly dependent on them, it is necessary to use other experimental parameters to determine them.

The information bearing on these coordinates is the upper limit of $0.6D$ on μ_{\perp} , which depends on ϕ_d , as well as θ_a and θ_d , and the $K=2$ doubling constants, Table 1, which are strongly affected by χ_a , χ_d and ϕ_d . Using a vector model, as in Eq. 1, but dropping the enhancement terms which will be negligible for the purpose of this calculation,

$$\mu_{\perp} \cong \mu [\sin^2 \theta_a + \sin^2 \theta_d + 2 \sin \theta_a \sin \theta_d \cos \theta_d]^{1/2}$$

Thus μ_{\perp} changes monotonically from about $0.1D$ to $3.D$ as ϕ_d goes from $0-180^\circ$. For $\theta_a = 58^\circ$, $\theta_d = -51^\circ$ and $\mu_{\perp} \leq 0.6D$, a value of $\phi_d \leq 25^\circ$ is obtained.

The $K=2$ doubling constants depend on the term $(C-B)^2/16(2A-B-C)$ which is a strong function of χ_a , χ_d and ϕ_d , as shown in Table 12. In fact, if $\chi_a \approx \chi_d \approx \phi_d \approx 0$, $C-B$ is less than 5 MHz and water dimer is nearly an accidental symmetric top. If these angles differ from 0° , $C-B$, and $(C-B)^2/16(2A-B-C)$ rapidly increase (Table 12). As noted earlier, the experimental $K=2$ doubling constants do not have the correct isotopic dependence for a rigid rotor. Upon complete deuteration, $(C-B)^2/16(2A-B-C)$ should increase by about a factor of 5 rather than the slight decrease observed experimentally. Presumably dynamic effects involving centrifugal distortion (D_3 coefficient in the $K=2$ constant c) and vibrational averaging are causing the deviation from rigid-rotor behavior. Assuming that such dynamic effects will be smallest in $(D_2O)_2$, the $K=2$ doubling constants for that isotopic species can be used to set an approximate upper limit to the deviation of χ_d , χ_a and ϕ_d from zero degrees (the near symmetric top case). For $c_{E_2} = 1.7$ kHz, an upper limit of 30° for each angle is obtained (the corresponding limit for

$c_{E1} = 0.5$ kHz is only 15°). The situation becomes less clear if χ_d and χ_a are simultaneously varied. If χ_d and χ_a are both increased from zero $\frac{(C-B)^2}{16(2A-B-C)}$ remains very small, while if one angle becomes positive and the other negative, this quantity increases quite rapidly. It should be noted that $\chi_d = 0$ for a linear hydrogen bond so it is reasonable that χ_d and therefore χ_a should be $< 30^\circ$. The strongest statement based purely on experimental data is that the experimental $K=2$ doubling constants are consistent with values of χ_a , χ_d and $\phi_d = 0$, but do not give unambiguous limits for χ_a and χ_d .

The structural parameters in Table 10 represent an average structure in the sense that our experimental measurements are made in the ground vibrational state. The vibrational averages of the measured quantities will vary from those of the equilibrium structure and of different isotopic species. It is difficult to assess this effect in the absence of accurate vibrational potentials. However, the dipole moment component, μ_a , is constant within 3% for all isotopic species and rotational-tunneling states measured. A change of only 3° in θ_a or θ_d would cause this variation. Although moments of inertia and electric dipole moments have different operator dependence, it is reasonable that the equilibrium geometry of water dimer is within the error limits given in Table 10. By comparison, the much less strongly bound ArHCl (about 0.5 kcal/mole as opposed to 5 kcal/mole for $(H_2O)_2$) complex shows a nearly 25% increase in dipole moment upon deuteration.^{41,42} The Ar-Cl-H angle calculated from the dipole moment is 47.5° for ArHCl, 33.5° for ArDCl and the equilibrium value of this angle was thought to be $\approx 0^\circ$.

In summary, we find $R_{OO} = 2.976(10)\text{\AA}$, $\theta_a = 58^\circ(6)$ and $\theta_d = -51^\circ(6)$ from the average of the two rows of Table 10. From the perpendicular dipole moment analysis, the torsional angle $\phi_d < 30^\circ$. The assumption that the molecule has a plane of symmetry (Fig. 4), $\chi_a = \chi_d = \phi_d = 0$, is consistent with K=2 doubling constant data, although rigorous limits on χ_a and χ_d cannot be determined from the isotopic species studied to date (partially deuterated species can resolve this problem). If χ_d is assumed to be zero, the above value for θ_d gives the hydrogen bond as linear within $1^\circ \pm 6^\circ$.

DISCUSSION

A large number⁴ of ab initio calculations of the structure of water dimer have been performed, with basis sets of varying size, and in a few cases, with configuration interaction.⁴³ In general,² the calculations find water dimer to have the trans configuration with a plane of symmetry and a linear hydrogen bond. The exact values of the equilibrium geometrical coordinates vary from calculation to calculation. Calculations with large basis sets have generally given $R_{OO} = 3.00\text{\AA}$, $\theta_a = 25-58^\circ$ and a linear hydrogen bond, where this was not a constraint. The agreement with the experimental R_{OO} value of $2.98(1)\text{\AA}$ is excellent and the linear hydrogen bond is in good agreement with our value of $\theta_d = -51(6)^\circ$ since $\theta_d = -52.26^\circ$ (and $\chi_d = 0$) gives a linear hydrogen bond in our coordinate system. The calculated values of θ_a are only in moderate agreement with the experimental result of $58(6)^\circ$, with the calculated values generally being smaller than this (note ref. 4m, however). Our results concerning the perpendicular dipole moment and K=2 doubling

constants are compatible with the trans structure with a symmetry plane ($\phi_d = \chi_a = \chi_d = 0$). We have a reasonably good limit on ϕ_d , $\leq 30^\circ$, from μ_\perp . The results bearing on χ_a and χ_d are ambiguous, but if the hydrogen bond is assumed to be linear, $\chi_a = 0$, the K=2 doubling constants suggest that $\chi_d \leq 30^\circ$. In summary, we feel that the results of the more extensive ab initio calculations are in good agreement with experiment, except perhaps for θ_a .

Table 13 shows two interesting trends in this study of $(H_2O)_2$ and the earlier study on $(HF)_2$ of Dyke, Howard and Klemperer.³ In both of these molecules, the heavy atom internuclear distance is considerably longer in the dimer than in the corresponding solid phase. Frank⁴⁴ and others have discussed the idea that cooperative phenomena are important in hydrogen bonding. The results in Table 13 imply that hydrogen bonds in the solid phase are shorter and stronger than in the dimer. Apparently when a hydrogen bond is formed, charge transfer occurs in such a way as to enhance the formation of further hydrogen bonds. Presumably negative charge is transferred to the electronegative atom of the proton donor and positive charge to the hydrogens of the proton acceptor, strengthening the next hydrogen bond.

A second important point in Table 13 is the nearly tetrahedral directivity of the proton acceptor. It is not at all obvious that hydrogen bonds, which are weak compared to a normal covalent bond, should show this directionality.⁴⁵ For example, electron density maps do not show prominent lone pairs in H_2O or in HF , which has cylindrical symmetry in its charge distribution. Nevertheless, unless this result

is accidental, covalent bonding apparently plays an important role in the hydrogen bond, and in particular, in its stereochemistry. In regard to the important question of the change in orbital hybridization on hydrogen bonding, i.e., ice has local tetrahedral structure, but the H_2O bond angle is only 104.52° , our calculations are not sufficiently accurate for a definite answer. Studies of the partially deuterated water dimer, along with a more refined model, may prove to be successful in determining this question.

Appendix

To show that $(B+C)/2$ for $(H_2^{16}O)_2$ and $(H_2^{18}O)_2$ does not give reliable parameters, consider expanding $(B+C)/2$ in a Taylor series near the geometry given in tables 8 and 10. Retaining only linear terms gives:

$$\Delta(B+C)_{16}/2 = -4013\Delta R_{OO} + 4.05\Delta\theta_d + 4.18\Delta\theta_a$$

$$\Delta(B+C)_{18}/2 = -3631\Delta R_{OO} + 3.30\Delta\theta_d + 3.42\Delta\theta_a$$

$$\Delta(B+C)_D/2 = -3454\Delta R_{OO} + 6.47\Delta\theta_d + 6.31\Delta\theta_a$$

where the coefficients are calculated derivatives with units of MHz/A and MHz/degree. The derivatives for χ_a , χ_d and χ_d are all less than 0.05 MHz/degree and are neglected. The subscripts 16, 18 and D refer to $(H_2^{16}O)_2$, $(H_2^{18}O)_2$ and $(D_2^{16}O)_2$ respectively. The linear dependence of the $(H_2^{16}O)_2$ and $(H_2^{18}O)_2$ is better shown by dividing each equation by the coefficient of ΔR_{OO} :

$$[\Delta(B+C)_{16}/2]/4013 = -\Delta R_{OO} + 1.01 \times 10^{-3}\Delta\theta_d + 1.04 \times 10^{-3}\Delta\theta_a$$

$$[\Delta(B+C)_{18}/2]/3631 = -\Delta R_{OO} + 0.91 \times 10^{-3}\Delta\theta_d + 0.94 \times 10^{-3}\Delta\theta_a$$

$$[\Delta(B+C)_D/2]/3454 = -\Delta R_{OO} + 1.87 \times 10^{-3}\Delta\theta_d + 1.83 \times 10^{-3}\Delta\theta_a$$

Thus the coefficients of θ_a and θ_d in the first two of these equations differ by only 10%, while the equation for $(D_2O)_2$ has coefficients differing by a factor of two from the $(H_2O)_2$ equations. It is easily shown from these equations that if the $(B+C)/2$ values are in error by 10 MHz, e.g. because of zero point vibrational errors, the angles calculated from the $(H_2^{16}O)_2$ and $(H_2^{18}O)_2$ equations could be in error by 30°. If $(D_2O)_2$ and either of the $(H_2O)_2$ equations are used, an error of only 3° would result from a 10 MHz model error. $(B+C)/2$ actually de-

pende on the dimer coordinates in a non-linear fashion, but it is clear that the $(\text{H}_2^{16}\text{O})_2$ and $(\text{H}_2^{18}\text{O})_2$ data are not sufficiently independent to give reliable structural information in a simultaneous fit. A more accurate model, including vibrational averaging, will be necessary to use the $(\text{H}_2^{16}\text{O})_2$ and $(\text{H}_2^{18}\text{O})_2$ data together.

Acknowledgements

We would like to thank Keiji Morokuma for doing calculations on the dipole moment enhancement in water dimer and for many useful conversations. We also thank V. W. Laurie and W. A. Klemperer for lending us klystrons for some of the microwave measurements.

Footnotes

1. D. Eisenberg and W. Kauzmann, The Structure and Properties of Water, Oxford, New York (1969) Water, a Comprehensive Treatise, ed. by F. Franks, Plenum, New York (1972).
2. F. H. Stillinger, Adv. Chem. Phys. Vol. 31, 1 (1975).
3. T. R. Dyke, B. J. Howard, and W. A. Klemperer, J. Chem. Phys. 56, 2442 (1972).
4. a. K. Morokuma and L. Pedersen, J. Chem. Phys. 48, 3275 (1968)
b. J. Del Bene and J. A. Pople, J. Chem. Phys. 52, 4858 (1970)
c. K. Morokuma and J. R. Winnick, J. Chem. Phys. 52, 1301 (1970)
d. P. A. Kollman and L. C. Allen, J. Chem. Phys. 51, 3286 (1969)
e. D. Hankins, J. W. Moskowitz, and F. H. Stillinger, J. Chem. Phys. 53, 4544 (1970)
f. G. H. F. Diercksen, Theor. Chim. Acta. 21, 335 (1971)
g. M. J. T. Bowers and R. M. Pitzer, J. Chem. Phys. 59, 1325 (1973)
h. H. Popkie, H. Kistenmacher, and E. Clementi, J. Chem. Phys. 59, 1325 (1973)
i. H. Kistenmacher, H. Popkie, E. Clementi and R. O. Watts, J. Chem. Phys. 60, 4455 (1974)
j. H. Kistenmacher, G. C. Lie, H. Popkie, and E. Clementi, J. Chem. Phys. 61, 546 (1974)
k. G. H. F. Diercksen, W. P. Kraemer, and B. O. Ross, Theor. Chim. Acta 36, 249 (1975)
l. G. C. Lie and E. Clementi, J. Chem. Phys. 62, 2165 (1975)
m. L. A. Curtiss and J. A. Pople, J. Mol. Spec. 55, 1, 1975
n. O. Matsuoka, E. Clementi, and M. Yoshimine, J. Chem. Phys. 64, 1351 (1976)

- o. L. L. Shipman, J. C. Owicki, and H. A. Scheraga, J. Phys. Chem. 78, 2055 (1974)
- p. J. C. Owicki, L. L. Shipman, and H. A. Scheraga, J. Phys. Chem. 79, 1794 (1975)
- q. C. Braun and H. Leidecker, J. Chem. Phys. 61, 3104 (1974)
5. e.g. refs. 4b,e,p
6. G. C. Pimentel and A. L. McClellan, The Hydrogen Bond, p.33, W. H. Freeman, San Francisco (1960).
7. M. Van Thiel, E. Becker, and G. Pimentel, J. Chem. Phys. 27, 486 (1957).
8. A. Tursi and E. Nixon, J. Chem. Phys. 52, 1529 (1970).
9. F. T. Greene and T. A. Milne, J. Chem. Phys. 39, 3150 (1963).
10. J. Fricke, W. M. Jackson, and W. L. Fite, J. Chem. Phys. 57, 580 (1972).
11. T. R. Dyke and J. S. Muentner, J. Chem. Phys. 57, 5011 (1972).
12. T. R. Dyke and J. S. Muentner, J. Chem. Phys. 60, 2929 (1974).
12. a. T. R. Dyke, J. Chem. Phys. , (previous paper).
13. J. D. Anderson, R. P. Anders, and J. D. Fenn, Adv. Chem. Phys. 10, 275, 1966, and T. R. Dyke, G. R. Tomasevich, W. A. Klemperer, and W. E. Falconer, J. Chem. Phys. 57, 2277 (1972).
14. Drills purchased from Minatoc Tools, P. O. Box 10, New York, N.Y. 10014, Ni Foil purchased from A. D. McKay, 198 Broadway, New York, N.Y. 10038.
15. Transitions have been observed with $K \leq 5$. $K=5$ states have approximately 180 cm^{-1} of rotational energy.
16. We would like to thank the Pure Water Authority of Monroe County for providing starting material at nominal cost.
17. J. S. Muentner, J. Chem. Phys. 56, 5409, 1972 and R. E. Davis and J. S. Muentner, J. Chem. Phys. 61, 2940 (1974).

18. B. Fabricant and J. S. Muentner, J. Mol. Spec. 53, 57 (1974).
19. M. Kaufman, L. Wharton, and W. Klemperer, J. Chem. Phys. 43, 943 (1965).
20. General Scanning Inc., Watertown, Mass. Model G330.
22. C. H. Townes and A. L. Schawlow, Microwave Spectroscopy, Ch. 12, McGraw-Hill, New York (1955).
23. Ref. 1 Chapter 3.
24. A. H. Narten, J. Chem. Phys. 56, 5680 (1972).
25. The K-doubling is not necessarily symmetric about the average energy determined by $(B+C)/2$. Therefore, to extract $(B+C)/2$ from the average frequency of observed microwave doublets, small corrections should be made. The necessary information for the correction is contained in the radio frequency transition data, table 1. This correction is vanishingly small for $K \neq 2$. For details see ref. 22 eqs. 4-4, 4-6, and appendix III.
26. Ref. 22, p.87.
27. J. K. G. Watson, J. Chem. Phys. 46, 1935 (1967) and 48, 4517 (1968).
28. G. Winnewisser, J. Chem. Phys. 57, 1803 (1972).
29. Ref. 22, Chapter 10.
30. G. Herzberg, Spectra of Diatomic Molecules, p439, van Nostrand, New York (1950).
31. L. H. Scharpen, J. S. Muentner, and V. W. Laurie, J. Chem. Phys. 46, 2431 (1967).
31. a. J. S. Muentner, J. Chem. Phys. 56, 5409 (1972).
32. The u_a Stark effect for the $J=0$, $M=0 \rightarrow J=1$, $M=0$ and $J=1M=0 \rightarrow J=1M=1$ transitions will reflect a minimum of centrifugal distortion effects not only because of the low J values involved but also because both

Stark effects are dominated by the single $J=0 \rightarrow 1$ connection.

33. W. S. Benedict, N. Gailar, and E. K. Plyler, J. Chem. Phys. 24, 1139 (1956).
34. P. A. Kollman and L. C. Allen, J. Chem. Phys. 52, 5058 (1970) and J. Del Bene and J. A. Pople, J. Chem. Phys. 55, 2296 (1971).
35. Although this is presumably the lowest energy dimer structure, we note that even hexagonal (normal) ice has only a relatively small number of such configurations in its lattice.
36. T. R. Dyke and J. S. Muentner, J. Chem. Phys. 59, 3125 (1973).
37. A. D. Buckingham, Disc. Farad. Soc. 40, 232 (1965).
38. We would like to thank Keiji Morokuma for doing these calculations. An ST04-31G basis was used.
39. S. P. Liebman and J. W. Moskowitz, J. Chem. Phys. 48, 4544 (1968).
40. J. Verhoeven and A. Dymanus, J. Chem. Phys. 52, 3222 (1970).
41. S. E. Novick, P. Davies, S. J. Harris, and W. A. Klemperer, J. Chem. Phys. 59, 2273 (1973).
42. A. M. Dunker and R. G. Gordon, J. Chem. Phys. 64, 354 (1976).
43. See ref. 4n and references therein.
44. H. S. Frank and W. Y. Wen, Disc. Farad. Soc. 24, 133 (1957) and H. S. Frank, Proc. Roy. Soc. A247, 481 (1958).
45. We note that the HFF angle of $108(10)^\circ$ is almost consistent with the 120° FFF angle of crystalline HF as well as a tetrahedral angle (see refs. 3 and 47).
46. e.g. R_{OO} in heavy ice is given here; S. W. Peterson and H. A. Levy, Acta Crystallogr. 10, 70 (1957).
47. M. Atoji and W. N. Lipscomb, Acta Crystallogr. 7, 173 (1954).

Table 1. Radio Frequency Transitions

J	$(\text{H}_2\text{O})_2$			
	ν_{E_1} (MHz)	c_{E_1} (KHz) ^a	ν_{E_2} (MHz)	c_{E_2} (KHz) ^a
3 ^b			0.26	2.2
4 ^b	0.26	0.74	0.80	2.2
5	0.51	0.61	1.88	2.24
6	0.98	0.58	3.76	2.24
7	1.76	0.582	6.72	2.22
8	2.88	0.571	11.20	2.222
9	4.50	0.568	17.52	2.212
10	6.72	0.566	26.20	2.206
11	9.64	0.562	37.71	2.194
$(\text{D}_2\text{O})_2$				
5 ^b	0.42	0.50	1.40	1.67
6	0.76	0.45	2.90	1.73
7	1.40	0.463	5.20	1.72
8	2.30	0.456	8.65	1.72
9	3.60	0.455	13.55	1.711
10	5.43	0.457	20.30	1.709
11	7.82	0.456	29.29	1.707
12	11.05	0.460		

a. $c = [(B-C)^2/16(2A-B-C) + D_3]$.

b. Nonrandom errors greatly decrease the accuracy of c for very low frequency transitions.

Table 2. Data from Microwave Transitions $J, K \rightarrow J+1, K^a$

Species	J, K	Ave. Exp. Freq. (MHz)	Corrected ^b Freq. (MHz)
$(H_2^{16}O)_2 E_1$	0, 0	12 321.00	
	1, 0	24 640.88	
	2, 2	36 863.51	36 863.46
	3, 2	49 146.13	49 146.07
	3, 3	48 985.55	
$(H_2^{16}O)_2 E_2$	2, 2	36 928.57	36 928.45
	3, 2	49 232.47	49 232.23
	3, 3	49 205.54	
$(D_2^{16}O)_2 E_1$	2, 2	32 549.20	32 549.18
	3, 2	43 395.24	43 395.19
	3, 3	43 325.70	
$(D_2^{16}O)_2 E_2$	2, 2	32 564.58	32 564.50
	3, 2	43 415.58	43 415.41
	3, 3	43 366.63	
$(H_2^{18}O)_2 E_1$	2, 2	33 333.0	c
	3, 2	44 440.2	c
	3, 3	44 297.2	
$(H_2^{18}O)_2 E_2^d$	2, 2	33 384.5	c
	3, 2	44 507.8	c
	3, 3	44 301.5	

- a. Experimental uncertainties are in least significant figure quoted.
b. Corrections applied to the average of the two K doublet frequencies generate frequencies dependent only on $(B+C)/2$, see ref. 25. These corrections are vanishingly small for all but $K=2$ transitions.
c. Insufficient data are available for corrections to be made.
d. There are uncertainties in the assignment of $E_2^{18}O$ frequencies.

These data are included only for completeness and assignment may be in error.

Table 3. Properties Calculated from K=2,3 Microwave Frequencies

Species		$[(B+C)/2]_{00}$ (MHz)	D_J (KHz)	ω (cm ⁻¹)	D_{JK} (MHz)
$(H_2^{16}O)_2$	E ₁	6 160.8	46.7	149	4.01
	E ₂	6 158.3	50.1	143	0.67
$(D_2^{16}O)_2$	E ₁	5 432.4	33.1	147	1.74
	E ₂	5 432.9	35.0	143	1.22
$(H_2^{18}O)$	E ₁ ^a	5 570.4	34.1	149	3.57

a. D_{JK} given here depends on E₁ assignment, see text. E₂ assignments are uncertain for $(H_2^{18}O)_2$, see text and table 2.

Table 4. Least Squares fit Properties of $(\text{H}_2^{16}\text{O})_2 \text{ E}_1$.

$[(B+C)/2]_{00}$	=	6 160.7(1)	MHz
D_{JK}	=	4.01(1)	MHz
D_J	=	44(4)	KHz

Table 5. Dipole Moments^a for K=2,3 and 4 States

Species		J=2, K=2	J=3, K=2	J=3, K=3	J=4, K=4
(H ₂ O) ₂	E ₁	2.5881(5)	2.5843(5)	2.6238(8)	2.5835(10) ^b
	E ₂	2.6350(11)	-	2.5658(11)	2.5550(10) ^b
(D ₂ O) ₂ ^c	E ₁	2.6010(1)	-	2.6037(6)	-
	E ₂	2.6132(10)	-	2.5901(9)	-

a. Moments given in Debye measured relative to $\mu(\text{OCS}) = 0.71521$ (See ref. 31a). Figures in parentheses are one standard deviation in the precision, absolute accuracy is $\pm 0.02\%$.

b. J=4, K=4 cannot be assigned to specific E states.

c. E state assignment based on analogy with (H₂O)₂.

Table 6. K=0 Dipole Moment Data for $(\text{H}_2^{16}\text{O})_2$

$J, K, M \rightarrow J', K, M'$	Stark Coefficient ^a	C_2^b	μ^c (Debye)
0,0,0 \rightarrow 1,0,0	$[8\mu_a^2/15(B+C) + 2\mu_{\perp}^2/15A]E^2$	$7.66301(20) \times 10^{-5}$	2.64307(5)
1,0,0 \rightarrow 1,0, ± 1	$[3\mu_a^2/10(B+C) + \mu_{\perp}^2/5A]E^2$	$4.31197(30) \times 10^{-5}$	2.64354(10)
1,0,0 \rightarrow 2,0,0	$-[16\mu_a^2/105(B+C) + 4\mu_{\perp}^2/105A]E^2$	$-2.19409(80) \times 10^{-5}$	2.64588(75)

a. See text for definitions and assumptions.

b. Data was fit to the form $\nu = C_0 + C_2 E^2 + C_4 E^4$. C_4 was calculated and C_0 and C_2 determined. C_2 is given in cgs units.

c. This moment obtained from C_2 and the first term in the listed "Stark Coefficient". Values are relative to $\mu(\text{OCS}) = 0.71521$ (see ref. 31a). Numbers in parentheses are one standard deviation in the precision; absolute accuracy is $\pm 0.02\%$.

Table 7. Water Monomer Properties Used in Obtaining
Water Dimer Structure Parameters

		Ref.
O-H equilibrium bond length	$r_e = 0.9572 \text{ \AA}$	33
H-O-H equilibrium angle	$\alpha_e = 104.52^\circ$	33
electric dipole moment	$\mu = 1.855 \text{ D}$	36
polarizability component	$\alpha_{XX} = 1.452 \text{ \AA}^3$	39
	$\alpha_{YY} = 1.226 \text{ \AA}^3$	39
	$\alpha_{ZZ} = 1.651 \text{ \AA}^3$	39
electric quadrupole moment	$\phi_{XX} = 0.13 \times 10^{-26} \text{ esu-cm}^2$	40
	$\phi_{YY} = -2.63 \times 10^{-26} \text{ esu-cm}^2$	40
	$\phi_{ZZ} = 2.50 \times 10^{-26} \text{ esu-cm}^2$	40

Table 8. R_{OO} and θ_a from $(\frac{B+C}{2})$ for two isotopic species. The $(\frac{B+C}{2})$ values are for $J=0$, $K=0$ and, for the sake of definiteness, the E_1 tunneling state. For reasons discussed in the text, the $(H_2^{16}O)_2$ and $(H_2^{18}O)_2$ results are considered to be unreliable.

Isotopic Species	R_{OO} \circ (Å)	θ_a (Degrees)
$(H_2^{16}O)_2$ and $(D_2^{16}O)_2$	2.980	60.7
$(H_2^{18}O)_2$ and $(D_2^{16}O)_2$	2.973	56.8
$(H_2^{16}O)_2$ and $(H_2^{18}O)_2$	3.000	82.2

Table 9. Electrostatic calculation of induced dipole moment at several geometries.

R_{OO}	θ_d	θ_a	$[\mu_{ind}]_a$	$[\mu_{ind}]_a + [\Delta\mu_{CT}]_a$ (<u>ab initio</u> , ref.38)
2.98	-52.2	58	0.42	0.53
2.98	-57.2	63	0.41	0.52
2.98	-47.2	53	0.42	0.53

Table 10. R_{OO} , θ_a , θ_d from $\frac{B+C}{2}$ values and Eq. 2. The error limits in parentheses are calculated by assuming the dipole moment enhancement to have an error of ± 0.30 .

Isotopic species	μ_a^a (Debye)	R_{OO} (Å)	θ_a (Degrees)	θ_d^b (Degrees)
$(H_2^{16}O)_2, (D_2^{16}O)_2$	2.60	2.980(10)	58.5(60)	-50.2(60)
$(H_2^{18}O)_2, (D_2^{16}O)_2$	2.60	2.973(10)	56.7(60)	-52.2(60)

a. $\mu_a = 2.60$ D for all isotopic species within 2%.

b. Note that for a linear hydrogen bond, $\theta_d = -52.26^\circ$.

Table 11. Variation of $\frac{B+C}{2}$ for $(H_2^{16}O)_2$ with angular coordinates. $R_{OO} = 2.980 \text{ \AA}$. Comparison of each geometry with the first shows that $\frac{B+C}{2}$ depends strongly on θ_d and θ_a , but considerably less so on ϕ_d , χ_d and χ_a .

χ_d Degrees	θ_d Degrees	χ_a Degrees	θ_a Degrees	χ_a Degrees	$\frac{B+C}{2}$ MHz
0	-52.26	0	58	0	6 150.9
0	-52.26	0	0	0	6 020.2
0	0	0	58	0	6 274.5
0	-52.26	0	58	90	6 122.1
0	-52.26	90	58	0	6 180.3
180	-52.26	0	58	0	6 160.3

Table 12. Variation of $(C-B)^2/16(2A-B-C)$ for $(D_2O)_2$.
 $R_{OO} = 2.980 \text{ \AA}$, $\theta_d = -52.26^\circ$, $\theta_a = 58^\circ$. This
parameter increases rapidly as ϕ_d , χ_d and χ_a
are (singly) varied from 0° . Note that if
both χ_a and χ_d are increased by the same
amount, $(C-B)^2/16(2A-B-C)$ remains small.

ϕ_d Degrees	χ_d Degrees	χ_a Degrees	$(C-B)^2/16(2A-B-C)$ KHz
0	0	0	0.0124
30	0	0	2.33
0	30	0	2.12
0	0	30	1.65
0	30	30	0.00771
0	30	-30	5.20

Table 13. H_2O and HF dimer heavy atom internuclear distances and their increases from that of ice and solid HF, respectively. The orientation of the proton acceptor molecule, θ_a , is given, as is the corresponding tetrahedral angle.

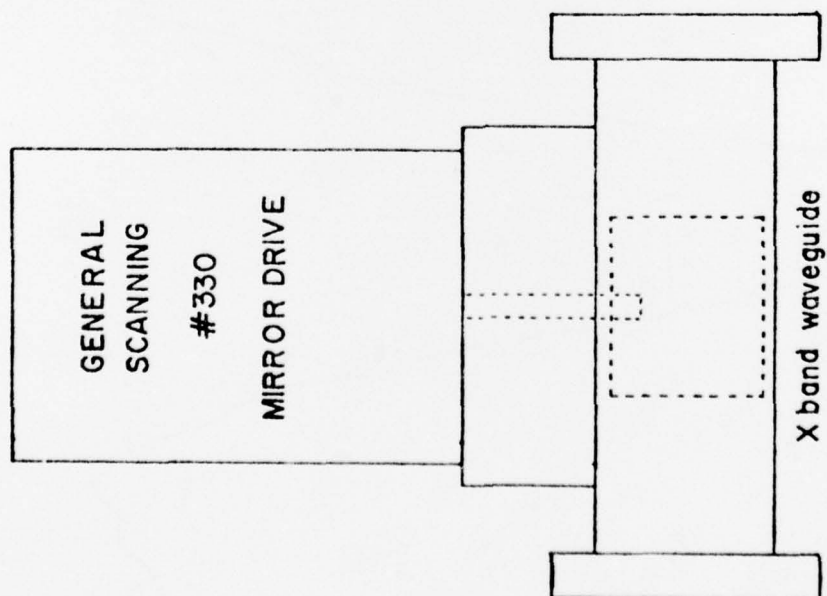
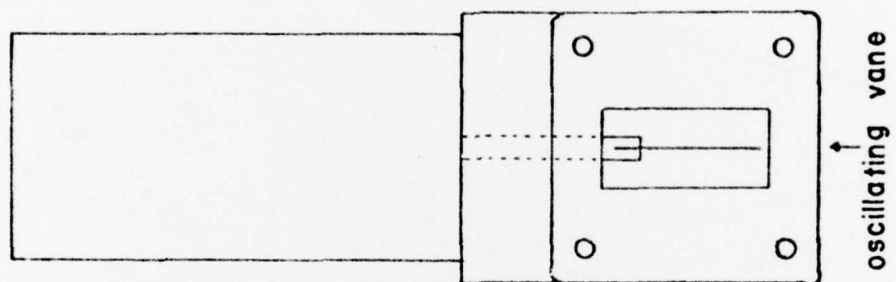
	R_{XX} ° (Å)	ΔR_{XX} ° (Å)	θ_a	" ϕ_T "
$(\text{H}_2\text{O})_2$	2.98(1)	0.22 ^a	58(6)°	54°44'
$(\text{HF})_2$	2.79 ³ (1)	0.30 ^b	108(10)°	109°28'

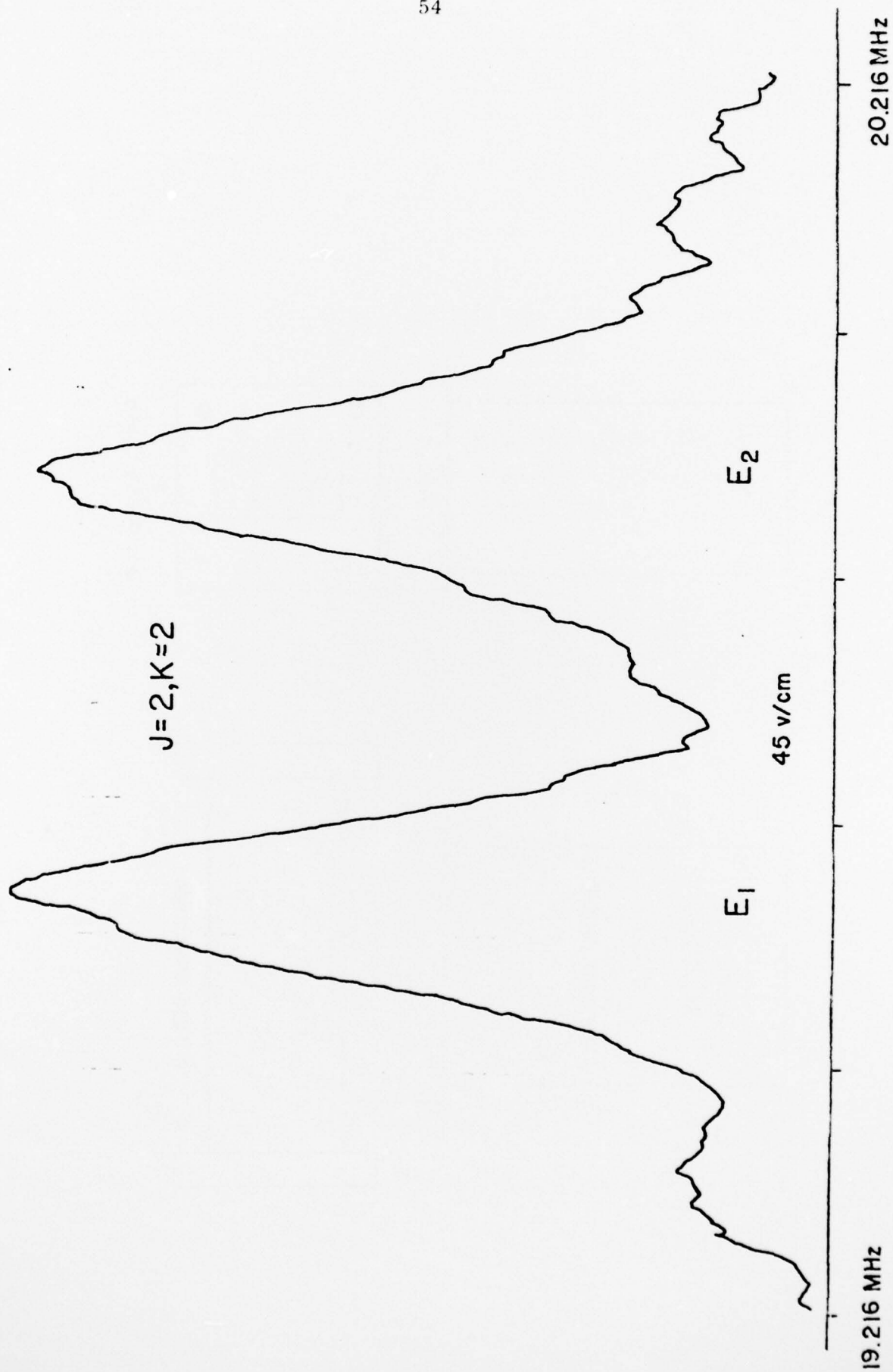
a. ref. 46.

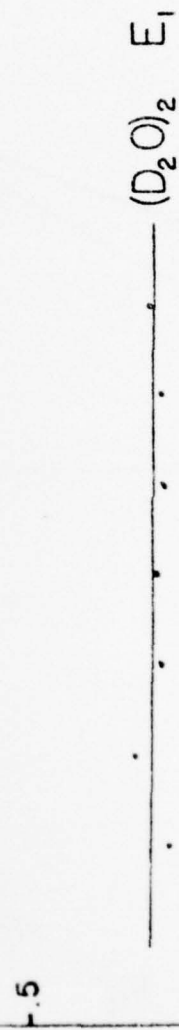
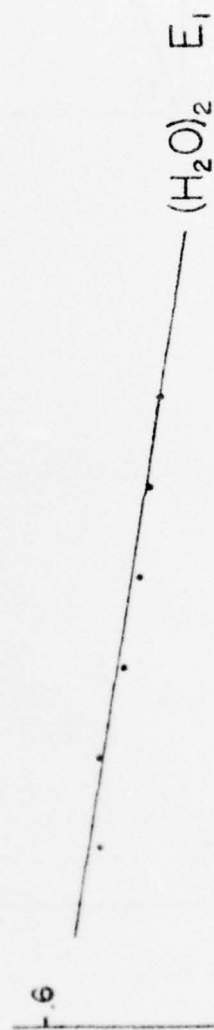
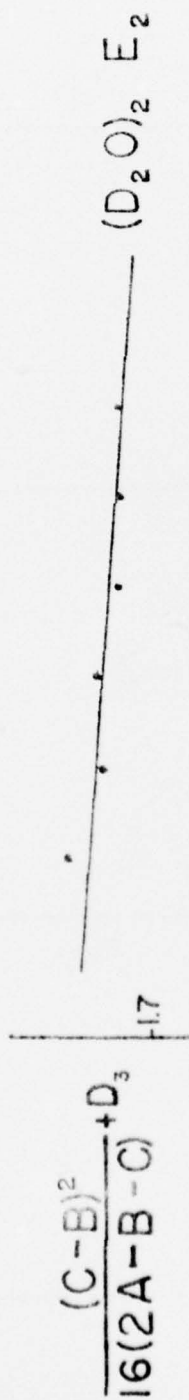
b. ref. 47.

Figure Captions

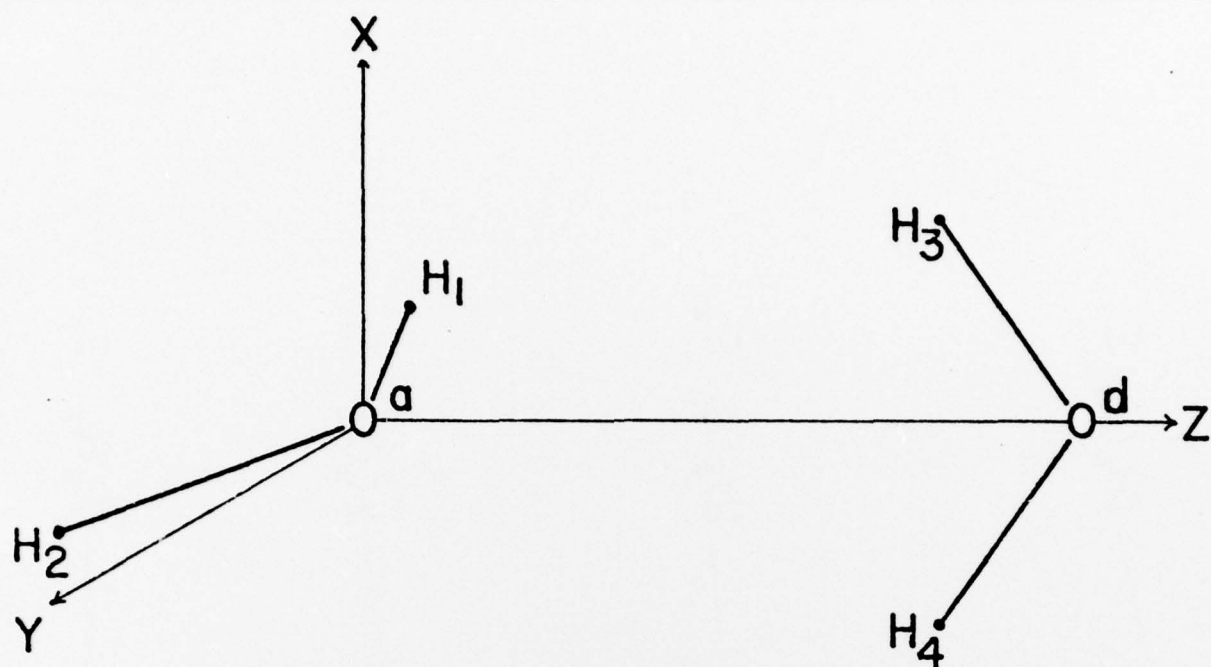
- Figure 1: Cross sectional views of mechanical microwave modulator.
- Figure 2: Pure Stark transitions for the E_1 and E_2 , $J=2$, $K=2$ states. These results were obtained using signal averaging with an effective time constant of 100 seconds. The linewidth includes unresolved hyperfine structure.
- Figure 3: Radio frequency $K=2$ transitions plotted as a function of J .
- Figure 4: a. Reference configuration for water dimer structure. The Y axis points toward the observer with the acceptor in the YZ plane and the donor in the XZ plane.
- b. Water dimer configuration. θ_a and θ_d give the angles made by the C_2 axis of the acceptor and donor monomers, respectively, with the Z (oxygen-oxygen) axis. The azimuthal angle ϕ_a is fixed at zero and ϕ_d then gives the torsional angle between the monomers. χ_a and χ_d specify the rotation about each monomer C_2 axis. $\chi_a = \chi_d = \phi_d = 0$ specifies a dimer with an XZ symmetry plane. A linear hydrogen bond has $\theta_d = -\frac{1}{2}\alpha$ and $\chi_d = 0$, where α is the monomer bond angle.



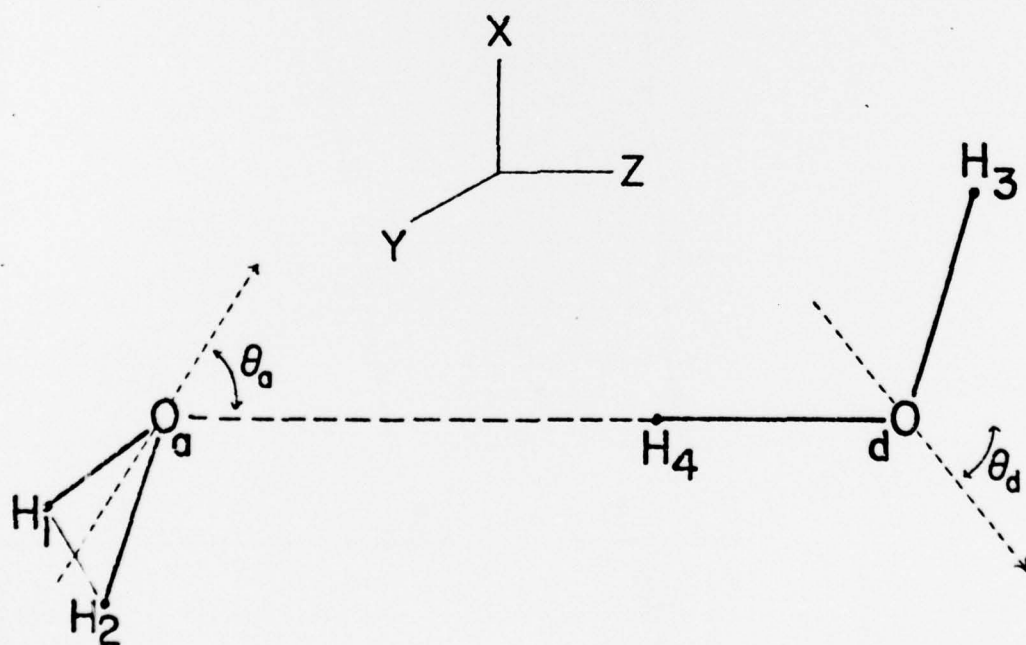




J



A



B